



**HAL**  
open science

# Simulations of the transport and deposition of $^{137}\text{Cs}$ over Europe after the Chernobyl Nuclear Power Plant accident: influence of varying emission-altitude and model horizontal and vertical resolution

Nikolaos Evangeliou, Yves Balkanski, Anne Cozic, Anders Pöpe Møller

## ► To cite this version:

Nikolaos Evangeliou, Yves Balkanski, Anne Cozic, Anders Pöpe Møller. Simulations of the transport and deposition of  $^{137}\text{Cs}$  over Europe after the Chernobyl Nuclear Power Plant accident: influence of varying emission-altitude and model horizontal and vertical resolution. *Atmospheric Chemistry and Physics*, 2013, 13 (14), pp.7183-7198. 10.5194/acp-13-7183-2013 . hal-02874085

**HAL Id: hal-02874085**

**<https://hal.science/hal-02874085>**

Submitted on 18 Jun 2020

**HAL** is a multi-disciplinary open access archive for the deposit and dissemination of scientific research documents, whether they are published or not. The documents may come from teaching and research institutions in France or abroad, or from public or private research centers.

L'archive ouverte pluridisciplinaire **HAL**, est destinée au dépôt et à la diffusion de documents scientifiques de niveau recherche, publiés ou non, émanant des établissements d'enseignement et de recherche français ou étrangers, des laboratoires publics ou privés.



# Simulations of the transport and deposition of $^{137}\text{Cs}$ over Europe after the Chernobyl Nuclear Power Plant accident: influence of varying emission-altitude and model horizontal and vertical resolution

N. Evangeliou<sup>1</sup>, Y. Balkanski<sup>1</sup>, A. Cozic<sup>1</sup>, and A. P. Møller<sup>2</sup>

<sup>1</sup>Laboratoire des Sciences du Climat et de l'Environnement (LSCE), CEA-UVSQ-CNRS UMR8212, Institut Pierre et Simon Laplace, L'Orme des Merisiers, 91191 Gif sur Yvette Cedex, France

<sup>2</sup>Laboratoire d'Ecologie, Systématique et Evolution, CNRS UMR8079, Université Paris-Sud, Bâtiment 362, 91405 Orsay Cedex, France

Correspondence to: N. Evangeliou (nikolaos.evangeliou@lsce.ipsl.fr)

Received: 23 October 2012 – Published in Atmos. Chem. Phys. Discuss.: 20 March 2013

Revised: 22 June 2013 – Accepted: 24 June 2013 – Published: 29 July 2013

**Abstract.** The coupled model LMDZORINCA has been used to simulate the transport, wet and dry deposition of the radioactive tracer  $^{137}\text{Cs}$  after accidental releases. For that reason, two horizontal resolutions were deployed and used in the model, a regular grid of  $2.5^\circ \times 1.27^\circ$ , and the same grid stretched over Europe to reach a resolution of  $0.66^\circ \times 0.51^\circ$ . The vertical dimension is represented with two different resolutions, 19 and 39 levels respectively, extending up to the mesopause. Four different simulations are presented in this work; the first uses the regular grid over 19 vertical levels assuming that the emissions took place at the surface (RG19L(S)), the second also uses the regular grid over 19 vertical levels but realistic source injection heights (RG19L); in the third resolution the grid is regular and the vertical resolution 39 levels (RG39L) and finally, it is extended to the stretched grid with 19 vertical levels (Z19L). The model is validated with the Chernobyl accident which occurred in Ukraine (ex-USSR) on 26 May 1986 using the emission inventory from Brandt et al. (2002). This accident has been widely studied since 1986, and a large database has been created containing measurements of atmospheric activity concentration and total cumulative deposition for  $^{137}\text{Cs}$  from most of the European countries.

According to the results, the performance of the model to predict the transport and deposition of the radioactive tracer was efficient and accurate presenting low biases in activity

concentrations and deposition inventories, despite the large uncertainties on the intensity of the source released. The best agreement with observations was obtained using the highest horizontal resolution of the model (Z19L run). The model managed to predict the radioactive contamination in most of the European regions (similar to De Cort et al., 1998), and also the arrival times of the radioactive fallout. As regards to the vertical resolution, the largest biases were obtained for the 39 layers run due to the increase of the levels in conjunction with the uncertainty of the source term. Moreover, the ecological half-life of  $^{137}\text{Cs}$  in the atmosphere after the accident ranged between 6 and 9 days, which is in good accordance to what previously reported and in the same range with the recent accident in Japan. The high response of LMDZORINCA model for  $^{137}\text{Cs}$  reinforces the importance of atmospheric modelling in emergency cases to gather information for protecting the population from the adverse effects of radiation.

## 1 Introduction

The Chernobyl Nuclear Power Plant (NPP) accident on 26 April 1986 resulted in the dispersion and deposition of a large amount of radionuclides into the environment. On 26 April 1986, two explosions took place in the power plant

releasing and transporting radioactive materials over long distances. The absence of reliable models in the period of the accident and the lack of reliable information (e.g. absence of national well-organised monitoring centres providing support to the official authorities) on the direction taken by the released elements motivated several researchers to develop environmental modelling tools, in order to be able to study potential accidental scenarios. Since then, many national and international efforts have been initiated to develop reliable models that will be able to describe transport and dispersion mechanisms when large amounts of radionuclides are released. Such tracer models can be used to estimate the spatiotemporal distribution of the fallout from accidental releases and the output can be used for preventive purposes, as well as to estimate the exposure and the harmful impacts from the dangerous compounds on humans, animals and vegetation.

It has been estimated that over  $10\text{ EBq}$  ( $\times 10^{18}\text{ Bq}$ ) of fission and activation products escaped from the damaged reactor (De Cort et al., 1998), whereas  $2\text{ EBq}$  (the most refractory) were deposited in the  $30\text{ km}$  vicinity of the power plant (Hatano et al., 1998). The most abundant nuclides were  $^{133}\text{Xe}$  ( $\sim 6500\text{ PBq}$ ),  $^{131}\text{I}$  ( $1200\text{--}1700\text{ PBq}$ ),  $^{132}\text{Te}$  ( $1000\text{--}1200\text{ PBq}$ ),  $^{137}\text{Cs}$  ( $\sim 85\text{ PBq}$ ),  $^{90}\text{Sr}$  ( $81\text{ PBq}$ ),  $^{134}\text{Cs}$  ( $44\text{--}48\text{ PBq}$ ), whereas the most refractory, less volatile radionuclides were  $^{144}\text{Ce}$ ,  $^{141}\text{Ce}$ ,  $^{106}\text{Ru}$ ,  $^{140}\text{Ba}$ ,  $^{95}\text{Zr}$ ,  $^{99}\text{Mo}$ ,  $^{238\text{--}241}\text{Pu}$  etc. (Devell et al., 1996; De Cort et al., 1998). However, a radionuclide of major concern is  $^{137}\text{Cs}$ , due to its half-life ( $30.2\text{ yr}$ ), the radiation type it emits during its radioactive decay and its bioaccumulation by organisms. Consequently, it is a chemical analogue of potassium and rubidium with high mobility in biological systems. Its chemical and metabolic-physiological reactions are similar to those of potassium (Woodhead, 1973) that is essential for many organisms. This explains why  $^{137}\text{Cs}$  gets enriched within tissues and cells. However, Cs cannot easily replace K in its metabolic functions, and it is not usually received by organisms in the same portion as potassium (Kornberg, 1961). Finally, it also participates in the augmentation of the total radioactivity to which the population is exposed.

Despite the dramatic consequences of the Chernobyl reactor accident, the atmospheric releases and the observed deposition of radionuclides provide a challenge for the modellers to test and improve their long-range dispersion models. For many years, operational codes have been developed to quantify the global fluxes of chemical pollutants (Elliassen, 1978; Elliassen and Saltbones, 1983; Prather et al., 1987; Lee et al., 2001; Stier et al., 2005; Koch et al., 2009; Huneus et al., 2011; Olivié et al., 2012). At the same time, some authors proposed the use of certain codes to analyse and/or predict the atmospheric transfer of radionuclides (ApSimon et al., 1985, 1987; Jacob et al., 1987, 1997; Albergel et al., 1988; Lange et al., 1988; Hass et al., 1990; Piedelievre et al., 1990; Balkanski et al., 1992; Klug et al., 1992; Ishikawa, 1995; Brandt et al., 2002; Quélo et al., 2007). It is well established

that such models provide a good description of the climatological long-range transport. However, the inconvenience in such studies arises from the fact that the simulations of the pollution episodes cannot be easily validated due to the lack of real-time qualitative measurements.

Many simulation studies have been performed in order to predict how the radioactive  $^{137}\text{Cs}$  migrated after the accident (e.g. Albeger et al., 1988; Hass et al., 1990; Bonelli et al., 1992; Desiato, 1992; Salvadori et al., 1996; Hatano et al., 1998; Brandt et al., 2002). The primary subject of these studies was emergency evacuation planning over regions within  $30\text{ km}$  from the site (called “the exclusion zone”), although most of the results were proven to be inconsistent with the measured data obtained afterwards. Today, more than  $25\text{ yr}$  after the accident, a better understanding of the fate of radionuclides has been obtained in terms of total deposition. Furthermore, high quality deposition measurements over Europe have become available from the Chernobyl period by the EU Joint Research Centre (JRC) called “the REM database”, whereas high resolution maps have been created called “Atlas of caesium deposition on Europe after the Chernobyl accident” (De Cort et al., 1998). These data have been continuously collected by the EU since 1986 in the frame of the REM (Radioactivity Environmental Monitoring) project presenting atmospheric activity concentrations and deposition inventories from European countries, and then used in this paper to validate the model ability to represent the spread and deposition of  $^{137}\text{Cs}$ . For the creation of the map (hereafter, referred to as the Atlas), the data have been corrected for radioactive decay to 10 May 1986. A similar map has also been published by Peplow (2006).

Consequently, the main goal of the present work was to study the efficiency of the model described here for the tracer  $^{137}\text{Cs}$  using the reported patterns of the Chernobyl releases and transportation over Europe. Therefore, (i) the altitude of the emissions after the episode was considered assuming that the emissions occurred (a) at the surface and (b) at several heights. Moreover, the resulting dispersion and deposition of  $^{137}\text{Cs}$  is presented using (ii) the regular grid ( $2.5^\circ \times 1.27^\circ$ ) and (iii) the zoom-version of the model. Finally, the results of the two versions are evaluated by using two different vertical resolutions: 19 and 39 vertical layers for the regular grid configuration. All the results have been compared with raw data from the REM database. Given the large global risk of human exposure to radiation, especially in areas around reactors in densely populated regions, notably in West Europe and South Asia, where a major reactor accident can expose around 30 million people to radioactive contamination (Lelieveld et al., 2012), a reliable transport model for radioactive substances would be a benefit. The recent decision by Germany (following the Fukushima Daiichi accident in Japan) to phase out its nuclear reactors will reduce the national risk, though a large risk will still remain from the reactors in the neighbouring countries.

## 2 Global atmospheric transport model

The aerosol module INCA (INteractions between Chemistry and Aerosols) is coupled to the general circulation model (GCM), LMDz, developed at the Laboratoire de Météorologie Dynamique in Paris, and the global vegetation model ORCHIDEE (ORganizing Carbon and Hydrology In Dynamic Ecosystems Environment) (LMDZORINCA) (see also Szopa et al., 2012). Aerosols and gases are treated in the same code to ensure coherence between gas phase chemistry and aerosol dynamics as well as possible interactions between gases and aerosol particles. The simulations using the regular grid described below were performed with a maximum horizontal resolution of 2.5 degrees in longitude and 1.27 degrees in latitude ( $144 \times 142$ ) (Fig. 1a). However, the GCM also offers the possibility to zoom over specific regions by stretching the grid with the same number of grid-boxes (Fig. 1b). In the present study the zoom version was used in Europe obtaining a maximum horizontal resolution of 0.6 degrees in longitude and 0.51 degrees in latitude. On the vertical dimension, the model uses sigma-p coordinates with 19 levels extending from the surface up to about 3.8 hPa corresponding to a vertical resolution of about 300–500 m in the planetary boundary layer (first level at 70 m height) and to a resolution of about 2 km at the tropopause (with 7–9 levels located in the stratosphere). Moreover, a vertical resolution of 39 layers has been installed and used extending from the surface up to the mesopause. More information about the parameterisation of wet and dry deposition can be found in the Supplement of this article (Methodology).

Each simulation was carried out for nine months (April to December 1986). Deposition of  $^{137}\text{Cs}$  in Europe one month after Chernobyl appeared to be at least two orders of magnitude, or more, lower than the maximum deposition just after the accident, and also that it was fractional (below detection limit) one year later (Kritidis, 1989). Therefore, nine months were sufficient to obtain more than 99 % of the  $^{137}\text{Cs}$  emitted. LMDZORINCA accounts for emissions, transport (resolved and sub-grid scale), photochemical transformations, and scavenging (dry deposition and washout) of chemical species and aerosols interactively in the GCM. Several versions of the INCA model are currently available depending on the envisaged applications with the chemistry-climate model. The model runs in a nudged mode (using the ERA40 Re-analysis data – 6 h wind fields – by the European Centre for Medium-Range Weather Forecasts, ECMWF, 2002) with a relaxation time of 10 days for the regular grid, whereas for the zoom version relaxing to 4.8 days in the centre of the zoom and to 10 days outside (Hourdin and Issartel, 2000).

The radioactive tracer  $^{137}\text{Cs}$  (half-life = 30.2 yr) was inserted as an inert tracer within the model. The behaviour of  $^{137}\text{Cs}$  in the atmosphere is strongly related to its chemical form as it may be released in the atmosphere in gaseous form or adsorbed onto particles. Here, it is assumed that mostly  $^{137}\text{Cs}$  behaves as an aerosol and as such it is treated

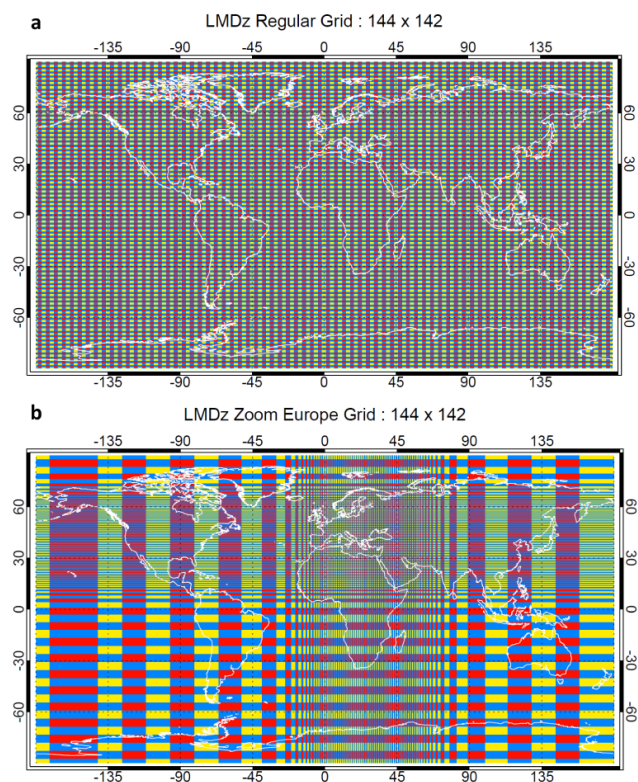


**Fig. 1.** (a)  $144 \times 142$  (points) regular grid of the GCM used for the simulations of the Chernobyl accident using 19 and 39 sigma-p vertical layers, (b)  $144 \times 142$  grid “stretched” over Europe (zoom-version) for 19 vertical layers.

in the model. In fact, this is true as it has been reported that over 80 % of the  $^{137}\text{Cs}$  emitted in the atmosphere during accidental releases is in the form of particulates (Richie and McHenry, 1990; Yoschenko et al., 2006; Sportisse, 2007; Morino et al., 2011; Potiriadis et al., 2011). The partitioning between gaseous form and particles and the size distribution of aerosols strongly affect dry deposition and scavenging.

## 3 Emission estimates after the accident

The coordinates of the emissions after the Chernobyl accident in the model were set to  $30.083^\circ\text{E}$  longitude and  $51.383^\circ\text{N}$  latitude. The precise amount of the emissions after the accident is still laden with uncertainty for the researchers and the local authorities and, typically, an uncertainty of 50 % is used in such analyses (e.g. Albeger et al., 1988; Hass et al., 1990; Brandt et al., 2002). The total source term evaluated by the ex-USSR authorities and published at an IAEA conference in 1986 (Hass et al., 1990) presented a value of  $37 (\pm 50\%) \text{ PBq}$  for  $^{137}\text{Cs}$  estimated on the basis that all the emitted  $^{137}\text{Cs}$  had been deposited in ex-USSR countries only. Nevertheless, a subsequent estimation of the activity of  $^{137}\text{Cs}$  emitted after the accident, taking into account the



amount of  $^{137}\text{Cs}$  deposited in all countries, showed a value more than 2 times higher ( $85 \pm 50\%$  PBq), which is 30 % of the total core inventory of  $^{137}\text{Cs}$  (280 PBq) (IAEA, 2006). The daily emission percentages (with respect to the total release), the respective activities and the injection height over 19 and 39 vertical layers can be found in Table 1. The major part of the initial emissions from Chernobyl has been estimated to take place at relatively high altitudes. After a few days, the major parts of the emissions were released at lower altitudes below 1.5 km, and in the following days the concentrations were transported over most of Europe with major influences in southern, eastern and central Europe. As a result of the two explosions held during the first day of the accident, the initial large release was due to the mechanical fragmentation of the fuel. It mainly contained the more volatile radionuclides such as noble gases, iodine and some caesium. The second large release in the end of this period was caused by the high temperatures reached in the core melt (Waight et al., 1995).

## 4 Results and discussion

### 4.1 Fallout transport over Europe using different model versions

Three separate simulations in the regular grid version of the model were performed, the first one assuming that all the amount of  $^{137}\text{Cs}$  was introduced at the site's surface (RG19L(S)), the second following the real emission altitude according to Table 1 spread over 19 layers (RG19L) and the final one over 39 layer resolution following the same emission patterns (RG39L). Moreover, one additional run was performed after installing the zoom-version of the model, stretched over Europe gridded within 19 vertical layers (Z19L) using the emissions denoted in Table 1. The  $^{137}\text{Cs}$  activity concentrations in Figs. 2–5 are expressed in Becquerel per  $\text{m}^3$  STP, where  $\text{m}^3$  STP is a standard cubic metre of air at 273.15 °K and 1 atm.

The atmospheric activity concentrations of  $^{137}\text{Cs}$  from the first run (RG19L(S)) are illustrated in Fig. 2 for the first day of the accident (26 March 1986), for the end of March (30 April 1986), as well as for 5 and 10 May 1986, in order to assess the direction of the radioactive fallout. It is noteworthy that the direction of the radioactive fallout seems not to vary much, mostly affecting the southern countries of Europe and the regions located in northern Africa. The atmospheric burden of  $^{137}\text{Cs}$  was found to be maximum on the last day of the emission (5 May reaching 24 PBq, which corresponds to 28 % of the total emitted (Table 2), and then decreased exponentially, presenting an ecological half-life for  $^{137}\text{Cs}$  of approximately 3 days (Fig. 6). The ecological half life of  $^{137}\text{Cs}$  is defined as the period of time it takes for  $^{137}\text{Cs}$  burden to decrease by half, affected by processes others than its radioactive decay (radioactive decay of  $^{137}\text{Cs}$  during the

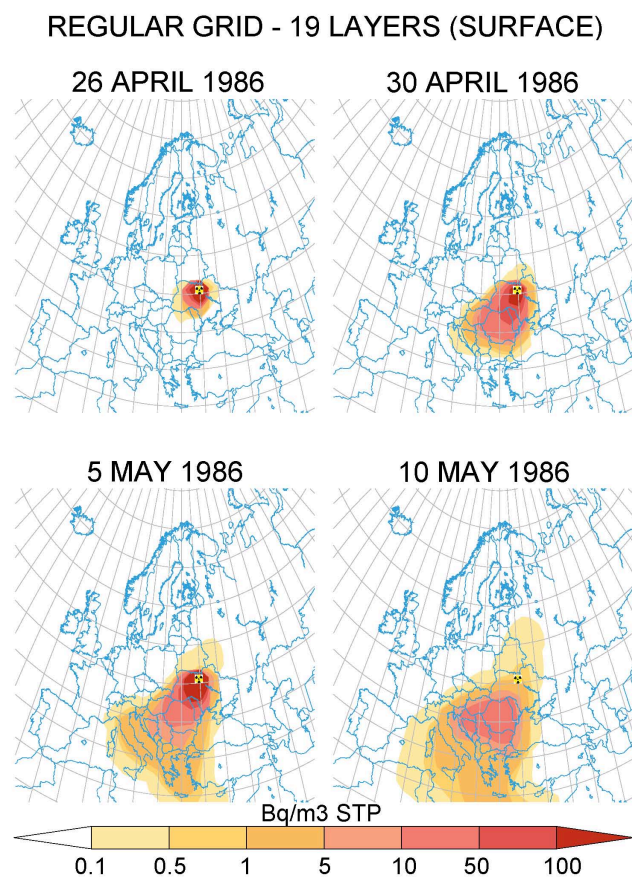


**Fig. 2.** Daily mean surface  $^{137}\text{Cs}$  activity concentrations (in  $\text{Bq m}^{-3}$  STP) from the Chernobyl accident. Model with regular grid and 19 vertical levels assuming surface emissions (RG19L(S)). The figures show the situation during the first day (26 April 1986), at the end of April (30 April 1986), the last day of the emissions (5 May 1986) and on 10 May 1986.

9 months runs was neglected since  $^{137}\text{Cs}$  is a long-lived radionuclide presenting a half-life of 30.2 yr. Consequently, during the last day of the emissions 28 % of  $^{137}\text{Cs}$  was still present in the atmosphere, whereas at the end of May the respective rate was 1.1 % (1.0 PBq) (Table 2). However, according to the REM database and previous simulations of the accident (e.g. Brandt et al., 2002) the direction depicted by this simulation is inaccurate. This result was expected since the prevailing winds at the surface blow in a very different direction than the ones above.

A closer representation of what happened after the accident is reflected by the second run of the model (RG19L) performed after introducing the known sources of  $^{137}\text{Cs}$  at different vertical layers of the model (see Table 1). This simulation indicates that the prevailing advective conditions have spread the radioactive fallout over longer distances than if emission occurred at the surface from the first day of the accident (Fig. 3). At the end of April 1986 the fallout was divided along three axis. The first one was transported to the

**Table 1.** Daily emissions of  $^{137}\text{Cs}$  in PBq after the Chernobyl accident in 1986 (according to Brandt et al., 2002) and relative vertical distribution in the model for 19 and 39 layers.

Mid-point in 19 Layers (m)	Layer thickness (m)	26 Apr (24 %)	27 Apr (8 %)	28 Apr (6.8 %)	29 Apr (5.2 %)	30 Apr (4 %)	1 May (4 %)	2 May (8 %)	3 May (10 %)	4 May (14 %)	1 May (16 %)
140	45–235	–	–	1.450	1.000	0.850	0.850	1.700	2.150	3.050	3.500
360	236–486	–	0.335	2.900	2.000	1.700	1.700	3.400	4.300	6.100	7.000
690	486–895	–	3.735	1.450	1.000	0.850	0.850	1.700	2.150	3.050	3.500
1200	896–1505	14.050	2.700	–	–	–	–	–	–	–	–
1900	1506–2295	5.050	–	–	–	–	–	–	–	–	–
2900	2296–3505	1.000	–	–	–	–	–	–	–	–	–
Mid-point in 39 Layers (m)	Layer thickness (m)	26 Apr (24 %)	27 Apr (8 %)	28 Apr (6.8 %)	29 Apr (5.2 %)	30 Apr (4 %)	1 May (4 %)	2 May (8 %)	3 May (10 %)	4 May (14 %)	1 May (16 %)
208	0–243	–	–	0.580	0.400	0.340	0.340	0.680	0.860	1.220	1.400
278	244–326	–	–	0.725	0.500	0.424	0.424	0.850	1.075	1.526	1.751
372	327–443	–	0.134	1.305	0.900	0.765	0.765	1.531	1.934	2.745	3.150
508	444–609	–	0.134	1.160	0.800	0.680	0.680	1.361	1.719	2.440	2.800
700	610–841	–	1.748	1.232	0.850	0.722	0.722	1.446	1.828	2.593	2.975
963	842–1154	1.405	1.681	0.652	0.450	0.382	0.382	0.765	0.968	1.373	1.576
1309	1155–1567	11.24	1.994	0.145	0.100	0.085	0.085	0.170	0.215	0.305	0.350
1754	1568–2095	3.425	1.080	–	–	–	–	–	–	–	–
2308	2096–2755	2.020	–	–	–	–	–	–	–	–	–
2982	2756–3562	1.610	–	–	–	–	–	–	–	–	–
3779	3563–4522	0.400	–	–	–	–	–	–	–	–	–
<b>TOTAL</b>		<b>20.10</b>	<b>6.771</b>	<b>5.800</b>	<b>3.999</b>	<b>3.398</b>	<b>3.398</b>	<b>6.803</b>	<b>8.600</b>	<b>12.201</b>	<b>14.001</b>

**Table 2.** Atmospheric burden of  $^{137}\text{Cs}$  in PBq (with respect to the total emission of 85 PBq) estimated from the different model-versions used for the Chernobyl simulation. RG19L(S) denotes the simulation in the regular grid ( $144 \times 142$ ) assuming surface emissions, RG19L the regular grid with the real emission height, RG39L the regular grid with a 39 layer vertical resolution and Z19L the zoom-version over 19 vertical layers.

	26 Apr	30 Apr	5 May	31 May	20 Jun	31 Jul	31 Aug	30 Sep	31 Oct	30 Nov	31 Dec
RG19L(S)	8.4	13	24	1.0	0.1	0.04	0.02	0.02	0.01	< 0.01	< 0.01
RG19L	11	27	41	6.8	1.1	0.19	0.09	0.07	0.5	0.04	0.04
RG39L	10	29	54	7.1	1.3	0.28	0.18	0.16	0.14	0.13	0.13
Z19L	12	28	43	7.0	1.2	0.25	0.13	0.10	0.08	0.07	0.06

northern side of Europe, mostly affecting Sweden and Norway and the second part to the western side impacting Central Europe, whereas the final one has a northeastern direction affecting Russia, Belarus and Ukraine. These results at the end of April concur with the findings of other researchers (Albergel et al., 1988; Brandt et al., 2002; Hass et al., 1990). During the last day of the emissions (5 May 1986), it is evident that the fallout has been distributed over most of Europe. Comparing to the total emission of  $^{137}\text{Cs}$  after the accident, 48 % (41 PBq) of the  $^{137}\text{Cs}$  emitted remained in the atmosphere on 5 May 1986 (Table 2). This is an additional difference between the two runs, since the fallout seems to be deposited more locally if emitted at the surface than at greater heights. The ecological half-life of  $^{137}\text{Cs}$  in the at-

mosphere was estimated by the exponential decrease of the burden and it was found to be almost 6 days (Fig. 6). This differs significantly from the respective ecological half-life estimated during the previous run (RG19L(S), 3 days). Cambray et al. (1987) reported that following the Chernobyl accident, the exponential decline of the  $^{137}\text{Cs}$  concentrations indicated a residence half-time of 7 days for  $^{137}\text{Cs}$ , which concurs very well with the value found here. The fallout was transferred south-easterly after the end of the emissions, mainly to the Middle East, whereas it weakened up to 4 orders of magnitude by the end of May, with only 8 % (6.8 PBq) of the total  $^{137}\text{Cs}$  emitted still remaining in the atmosphere. The next months the atmospheric burden decreased reaching 0.04 PBq at the end of December, which corresponds to

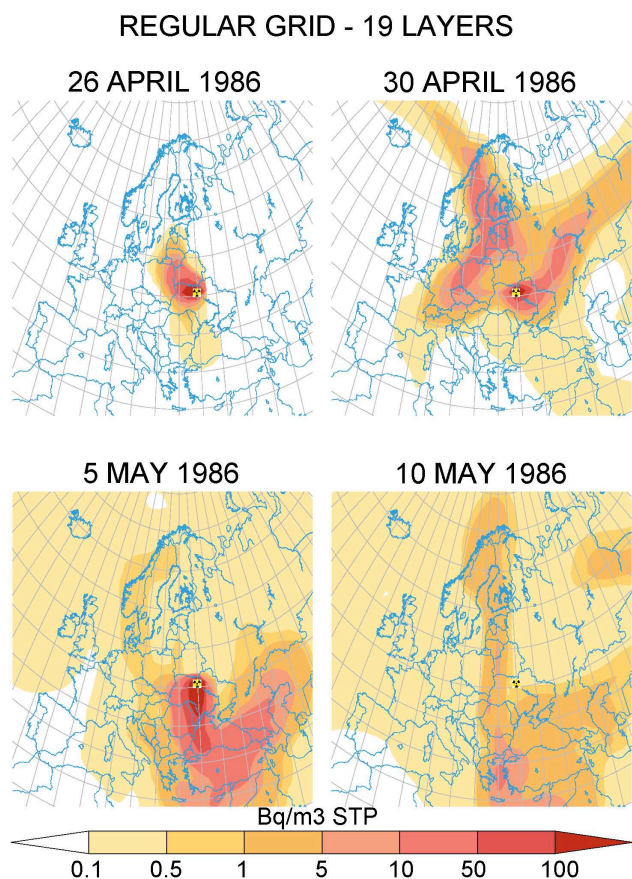


**Fig. 3.** Daily mean surface  $^{137}\text{Cs}$  activity concentrations (in  $\text{Bq m}^{-3}$  STP) from the Chernobyl accident. Model with regular grid and 19 vertical levels and injection at the real emission height (Table 1) (RG19L). The figures show the situation during the first day (26 April 1986), at the end of April (30 April 1986), the last day of the emissions (5 May 1986) and on 10 May 1986.

0.05 %, indicating that the vast majority of  $^{137}\text{Cs}$  has been deposited by the end of the year 1986 (Table 2). This is in good agreement with the measurements reported elsewhere (e.g. Ballestra et al., 1987; Mattsson and Vasanan, 1988).

Regarding the run performed after installing and using 39 layers in vertical resolution (RG39L) for the same horizontal resolution of the model, there were significant differences in the number of emission vertical levels. In this run the emission distribution in the vertical layers had more points, since the layers were separated by shorter distances between each other. However, the logic of choosing these amounts for each layer (as shown in Table 1) emanated precisely from the previous run (RG19L), in order to achieve similar amounts of  $^{137}\text{Cs}$  being emitted from similar altitudes as in the RG19L run. Despite the differences, the tendency of the fallout transport (Fig. 4) was the same as in the RG19L run, since the same ECMWF meteorology files are re-gridded respectively in the vertical plane for both RG19L and RG39L versions. For both resolutions transport occurs to North Europe on the

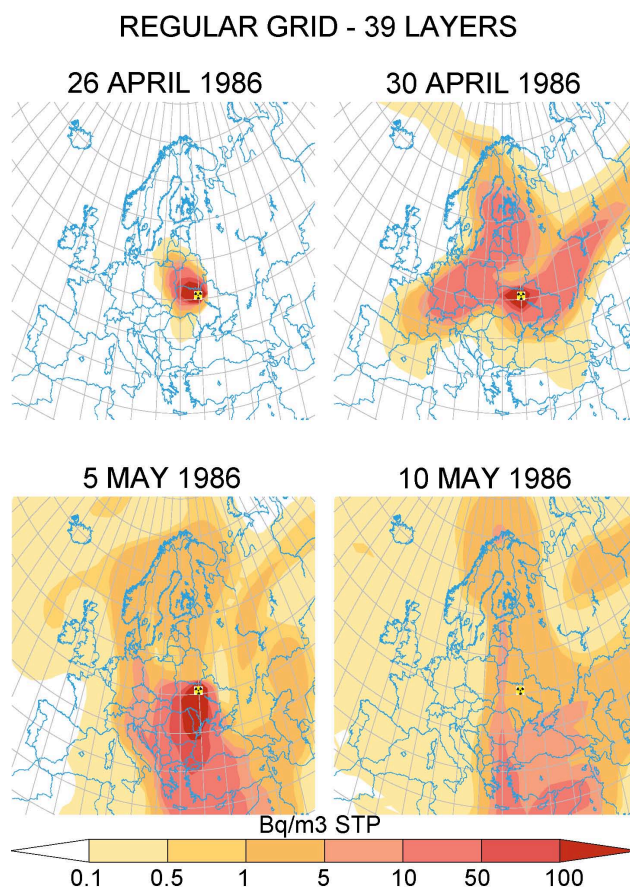


**Fig. 4.** Daily mean surface  $^{137}\text{Cs}$  activity concentrations (in  $\text{Bq m}^{-3}$  STP) from the Chernobyl accident. Model with regular grid and 39 vertical levels and injection at the real emission height (Table 1) (RG39L). The figures show the situation during the first day (26 April 1986), at the end of April (30 April 1986), the last day of the emissions (5 May 1986) and on 10 May 1986.

first day of emission (26 April), whereas the fallout was divided in three components on 30 May, one affecting North Europe (Sweden and Norway), a second one the Central European countries and a third one following a north-eastern direction (across Russia, Belarus and Ukraine). After the last emission date (5 May) the radioactive plume had been transferred across all Europe. The cyclone observed on 5 May north of the UK influences significantly the wind direction and has been reported by previous investigators in the area. The ecological half-life of  $^{137}\text{Cs}$  was estimated to be 9 days, which is higher than for the RG19L run (Fig. 6). In fact, in this run  $^{137}\text{Cs}$  was present for longer times in the atmosphere; the burden of  $^{137}\text{Cs}$  was estimated at 54 PBq (64 %) on 5 May, while the next months decreased exponentially reaching 0.13 PBq (0.15 %) at the end of 1986.

The same simulation for the Chernobyl accident was performed, after setting up a zoom-version of the model for 19 vertical layers (Z19L), centred over Europe. The initial transport (26 April) of the radioactive fallout shows a more



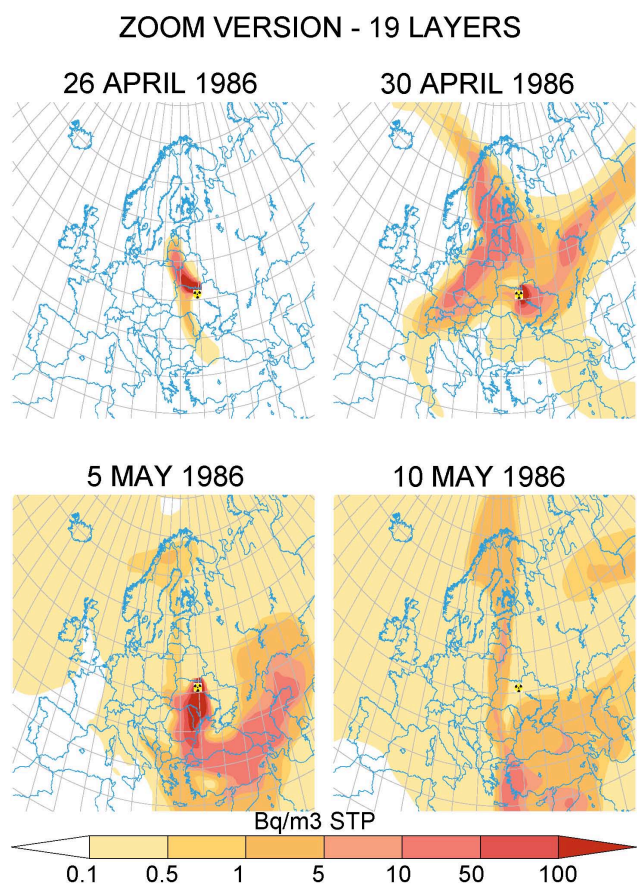


**Fig. 5.** Daily mean surface  $^{137}\text{Cs}$  activity concentrations (in  $\text{Bq m}^{-3}$  STP) from the Chernobyl accident. Model with regular grid stretched over Europe and 19 vertical levels and injection at the real emission height (Table 1) (Z19L). The figures show the situation during the first day (26 April 1986), at the end of April (30 April 1986), the last day of the emissions (5 May 1986) and on 10 May 1986.

pronounced meridional axis than in the previous simulations directed towards West-central Belarus (north), while a much weaker amount of  $^{137}\text{Cs}$  (more than two orders of magnitude less) was transferred to Romania and the Black Sea (south) (Fig. 5). The same transport trends have been validated and reported elsewhere (e.g. Brandt et al., 2002, Hass et al., 1990). At the end of April the three different directions of the plume (north, west, northeastern) were apparent and the respective levels were similar to the regular grid runs. On 5 May (last day of the emissions), the plume seems more intense in areas close to the source presenting a more local-based transport, with the fallout extending mostly to the east.  $^{137}\text{Cs}$  affects the central and eastern European regions, while it has not been transferred to Spain, Portugal and the north-east African countries yet. Observations support this transport pattern as these countries have reported trace amounts of  $^{137}\text{Cs}$  activity concentrations in the air or they were below the respective detection limits. The remaining  $^{137}\text{Cs}$  (burden)

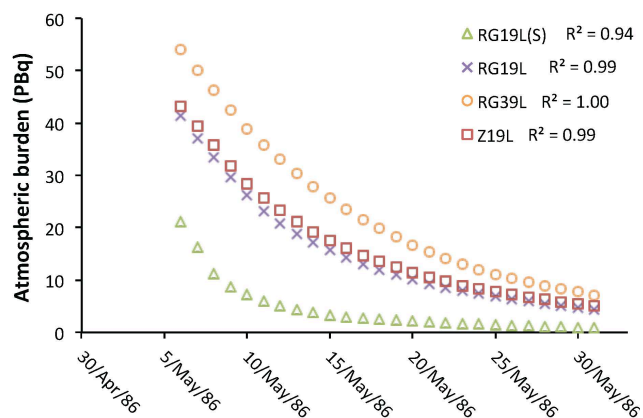


**Fig. 6.** Exponential decrease of the atmospheric burden of  $^{137}\text{Cs}$  (in PBq) for the 4 different simulations of the Chernobyl accident (RG19L(S), RG19L, RG39L and Z19L). This graph was used in order to estimate the ecological half-lives of  $^{137}\text{Cs}$  in the atmosphere.  $R^2$  is the correlation coefficient of the exponential fitting that the burden of  $^{137}\text{Cs}$  in the atmosphere follows.

was maximum on 5 May as it was estimated to be 43 PBq in the atmosphere, which corresponds to 51 % of the direct total emission (Table 2). The ecological half-life of  $^{137}\text{Cs}$  was also estimated to be almost 6 days (Fig. 6), which is comparable to those estimated by the previous runs and similar to those reported previously for the Chernobyl accident. However, a recent study following the Fukushima NPP accident in Japan showed ecological half-lives of  $^{137}\text{Cs}$  to be between 5 and 10 days (Kristiansen et al., 2012). Until 10 May the fallout appeared to follow a southern direction affecting the Middle East, just as in the previous simulations. During the last two thirds of May the radioactive plume over Europe was of the order  $\text{mBq m}^{-3}$  STP, whereas at the end of the month only 8.2 % (7.0 PBq) of the  $^{137}\text{Cs}$  emitted still resided into atmosphere. Likewise,  $^{137}\text{Cs}$  decreased in the following months and more than 99.9 % had been deposited by the end of 1986 (Table 2).

A three dimensional illustration of the  $0.15 \text{ Bq m}^{-3}$  STP iso-surface of  $^{137}\text{Cs}$  on 28 April (12:00 UTC) for 19 (left panel) and 39 vertical layers (right panel) is shown in Fig. 7 as in Brandt et al. (2002). The figure shows what can be seen from the south and  $^{137}\text{Cs}$  surface activity concentrations are plotted on the iso-surface. It is noteworthy that some parts of the plume experience vertical transport to higher altitudes. Another important feature here is the fact that the plume is distributed irregularly, both vertically and horizontally, in the 39 layers. It dominates the higher layers of the atmosphere across all Europe, in contrast to the 19 layers run, where the plume ascends mostly near the source. This is actually what Brandt et al. (2002) have proposed: parts of the plume are transported to higher altitudes where the wind direction is opposite to the direction found at lower levels. This wind pattern causes a transport in opposite horizontal directions



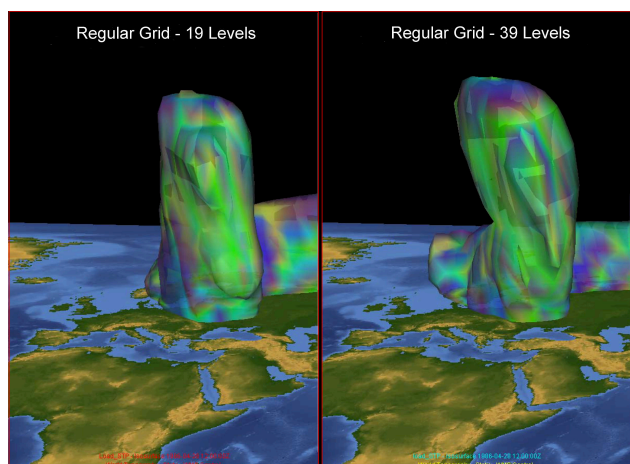


**Fig. 7.** A three-dimensional mapping of the  $0.15 \text{ Bq m}^{-3}$  STP iso-surface of  $^{137}\text{Cs}$  on the third day after the Chernobyl accident (28 April, 12:00 UTC) for 19 (left panel) and 39 vertical levels (right panel). Surface activity concentrations in  $\text{Bq m}^{-3}$  STP are plotted on the iso-surface with the darker colour indicating high concentrations and the lighter lower ones).

at different altitudes, i.e. towards northwest at lower altitudes and towards southeast at higher altitudes. The distribution of  $^{137}\text{Cs}$  on 28 April extends up to 388 mbars in the 19 layers and up to 74 mbars in the 39. It is obvious that larger amounts of  $^{137}\text{Cs}$  have been transferred to higher altitudes in the 39 levels (yellow colours in the iso-surface especially northerly – Fig. 7) resulting to higher residence times of  $^{137}\text{Cs}$  in the atmosphere (see Fig. 6). The Gaussian vertical motion in conjunction with the larger number of the levels spread the radionuclide into higher altitudes, despite our attempts of emitting similar amounts of  $^{137}\text{Cs}$  from similar heights in the model.

#### 4.2 Comparison with direct measurements of atmospheric activity concentrations

Data obtained from the four different runs of the Chernobyl accident were compared to real-time measurements of the activity concentrations of  $^{137}\text{Cs}$ . For that purpose, the aforementioned REM database was used. The activity concentrations from the database were divided in three parts according to the regions mostly affected by the radioactive fallout on 30 April 1986 (see Figs. 2–5), (a) West-central, (b) North and (c) South Europe. Time series measurements of  $^{137}\text{Cs}$  atmospheric concentrations between April and May 1986 can be found in Supplement, Fig. S1 for the regions examined.

In West-central Europe (Germany, France, UK, Belgium, Switzerland, Austria and Netherlands), the trends of  $^{137}\text{Cs}$  dispersion in the countries examined showed satisfactory results, in terms of activity concentrations and residence times as well (Supplement, Fig. S1). However, relatively small inaccuracies were observed on some days (e.g. in Austria

and Switzerland). The precision of the measurement technique used is not indicated in the database. Data from the REM database have been collected using several different techniques (e.g. direct airborne gamma spectrometry, surface pumping through disc filters followed by gamma spectrometry, etc.) and the specific method used at each station is not specified in the database. Therefore, determination recoveries contrast between different methodologies and this might induce additional uncertainties to the results. Regarding the residence time of  $^{137}\text{Cs}$  in the countries presented here, the model also shows robustness since, in most of the cases, similar levels were observed. Finally, the ending dates of the fallout, where  $^{137}\text{Cs}$  activity concentrations were near the limit of detection (LOD), concur with those of the model.

Similar results were found for the countries of North Europe (Finland, Norway, Sweden and Denmark) with smaller discrepancies (Supplement, Fig. S1). The most apparent were observed for Finland and Norway during the first days of May 1986, where the model underestimates the activity concentrations of  $^{137}\text{Cs}$ . However, the patterns of  $^{137}\text{Cs}$  activity concentrations in all cases were undoubtedly consistent indicating high accuracy for the model. Very similar levels were observed for the starting and the ending point of the radionuclide passage over the countries studied.

Finally, reliable results were obtained for South European countries (ex-Czechoslovakia, Hungary, Italy and Greece) (Supplement, Fig. S1), albeit underestimations over the Italian territory and overestimations over Greece. It is also essential to focus on another source of uncertainty. Even nowadays the exact emissions from the Chernobyl accident are unknown. Therefore, the relatively large discrepancy in the dosages of  $^{137}\text{Cs}$  can be explained from discrepancies in the source term or uncertainties in the effective release heights, since the injection altitudes used in the present study are only educated guesses. We state that they are “educated guesses” because (a) an uncertainty of at least  $\pm 50\%$  is used, and (b) the altitude of the emissions (which is very important and can change the transport regime extremely (as shown in the RG19L(S) simulation) is based on simple assessments. The last is mainly because tools such as back trajectories were not available 27 yr ago, and also, there was lack of information, while the national monitoring systems of the countries were not well developed like nowadays. Injection height seems to be very essential in terms of transport and deposition of  $^{137}\text{Cs}$  in certain regions. Another noteworthy point that we should focus on here is what we learn from the results of the RG19L(S) simulation, where surface emissions were assumed. These results differ significantly from measurements and also model-versions where real emission altitudes were used. For instance, no  $^{137}\text{Cs}$  was detected in North Europe until the end of May or extreme amount were estimated in South Europe at the start of the same month. This is additional evidence of how the exact height of the emission could affect the subsequent transport of  $^{137}\text{Cs}$  and the importance of the uncertainty induced by the source term.

**Table 3.** Comparison of the activity concentrations of  $^{137}\text{Cs}$  from the Chernobyl accident between the REM database and the different model versions used (RG19L(S), RG19L, RG39L and Z19L). Spearman Rank Order and Kendall Tau correlations ( $R^2$ ) between the datasets ( $N = 711$ ) for 95 % confidence level ( $p < 0.05$ ).

	Spearman Rank Order correlation					Kendall Tau correlation					
	REM	RG19L(S)	RG19L	RG39L	Z19L	REM	RG19L(S)	RG19L	RG39L	Z19L	
REM	<b>1.00</b>	0.21	0.64	0.61	0.62	REM	1.00	0.16	0.45	0.43	0.44
RG19L(S)	0.21	<b>1.00</b>	0.11	0.20	0.15	RG19L(S)	0.16	<b>1.00</b>	0.08	0.15	0.11
RG19L	0.64	0.11	<b>1.00</b>	0.84	0.84	RG19L	0.45	0.08	<b>1.00</b>	0.67	0.68
RG39L	0.61	0.20	0.84	<b>1.00</b>	0.72	RG39L	0.43	0.15	0.67	<b>1.00</b>	0.54
Z19L	0.62	0.15	0.84	0.72	<b>1.00</b>	Z19L	0.44	0.11	0.68	0.54	<b>1.00</b>

There are several numerical measures that quantify the extent of statistical dependence between pairs of databases. Here, we used the Spearman correlation method (Choi, 1977), which assesses how well the relationship between two variables can be described using a monotonic function. If there are no repeated data values, a perfect Spearman correlation of +1 or -1 occurs when each of the variables is a perfect monotone function of the other. Table 3 shows the respective results of the datasets compared (REM versus RG19L(S), RG19L, RG39L and Z19L, respectively) for the activity concentrations of  $^{137}\text{Cs}$ . According to the table, the Spearman correlation coefficient ranged from 0.61 to 0.64 for the runs where the emission altitude was taken into account for 95 % confidence level ( $p < 0.05$ ), whereas it was 0.21 for the RG19L(S) run; thus, the variables are statistically dependent. On the other hand, the data of the simulation with the real emission altitude are also highly dependent presenting coefficients of 0.84. For justification, Kendall rank correlation coefficient, commonly referred as Kendall's tau ( $\tau$ ) coefficient (Christensen, 2005) was also estimated (Table 3). This statistic measures the rank correlation, i.e. the similarity of the orderings of the data when ranked by each of the quantities. It is often used to test a statistical hypothesis in order to establish whether two variables may be regarded as statistically dependent. This test is non-parametric, as it does not rely on any assumptions on the distributions of  $X$  or  $Y$  ( $X$  and  $Y$  represent the variables under comparison). Under a "null hypothesis" of  $X$  and  $Y$  being independent, the sampling distribution of  $\tau$  will have an expected value of zero. Here, the  $\tau$  values were estimated to be around 0.44 for 95 % confidence level ( $p < 0.05$ ); thus, the "null hypothesis" can be rejected and the two datasets are dependent. The data derived from each simulation were very similar with  $\tau$  coefficients between 0.54–0.68. This can also be seen in Fig. 8, which depicts the Box and Whisker plot of the data. The range of the datasets for  $^{137}\text{Cs}$  activity concentrations is very similar, whereas the boxes corresponding to 25–75 % of the values were found at same level, although in some cases the model was found to underestimate. Besides statistics, the average relative biases were also calculated and presented in Supplement, Fig. S1 for each version except the one where surface

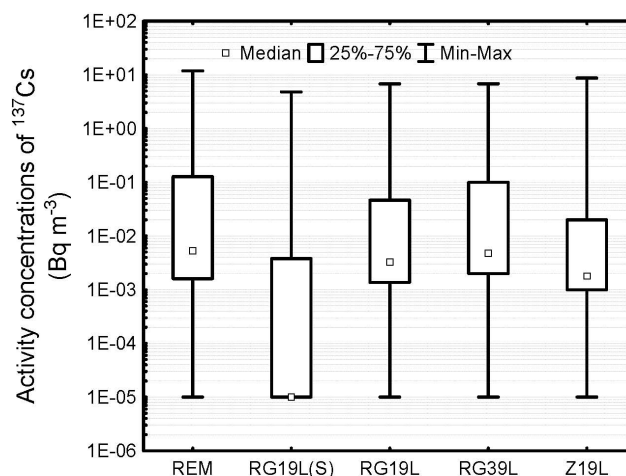


**Fig. 8.** Box & Whisker plots of the surface activity concentrations of  $^{137}\text{Cs}$  obtained from the REM database and from the simulations using all the available versions of the model. The plot depicts the smallest observation (sample minimum), lower quartile, median, upper quartile and the largest observation (sample maximum) ( $N = 711$ ).

emissions assumed. Despite the large variation in the biases, they present very satisfactory averages, 9.59, 81.49 and 3.81 for the RG19L, RG39L and Z19L run respectively, which are very good in comparison with previously reported ones for  $^{137}\text{Cs}$  activity concentrations of the Chernobyl accident (e.g. -61 in Brandt et al., 2002). The larger positive biases calculated for the 39 levels are a result of the elevation of higher amounts of  $^{137}\text{Cs}$  at greater heights (previously discussed in the manuscript) in conjunction with the resulting larger residence times.

Finally, the arrival times of the radioactive fallout of  $^{137}\text{Cs}$  were assessed for the four different simulations (RG19L(S), RG19L, RG39L and Z19L) and they were compared to those obtained from the REM database (REM). As arrival time we define the time after the accident it takes for  $^{137}\text{Cs}$  to reach the activity concentration of  $10^{-4} \text{ Bq m}^{-3}$  in a specific location, which is the minimum detected value of the REM database. The results are illustrated in a scatter plot

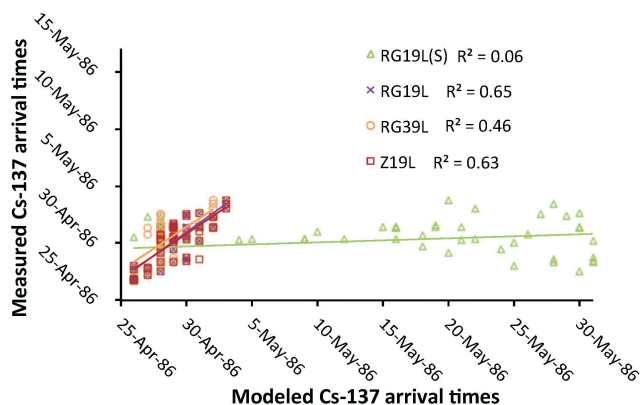


**Fig. 9.** Estimation of the arrival times of the radioactive fallout of  $^{137}\text{Cs}$  after simulation using all model versions (RG19L(S), RG19L, RG39L and Z19L) and comparison with the respective ones obtained from the REM database. The data correspond to time-series measurements from 56 sampling points across Europe.

in Fig. 9 for 56 measurement stations in 24 European countries (Ukraine, Russia, Poland, Romania, Hungary, Denmark, Belgium, Finland, Norway, Sweden, Germany, Netherlands, France, Italy, Great Britain, Austria, Switzerland, ex-Czechoslovakia, Turkey, Greece, Ireland, Egypt, Syria and Lebanon). The Pearson linear correlation coefficient was estimated to be 0.65 for the RG19L run, 0.46 for the RG19L and 0.63 for the Z19L, which is considered to be significant. The different vertical resolution resulted in a more rapid transport to the places examined. Moreover, as in the previous comparisons, the respective arrival times of  $^{137}\text{Cs}$  estimated from the regular grid run assuming surface emissions (RG19L(S)) were not reliable ( $R^2 = 0.08$ ). The model is able to predict the arrival times of  $^{137}\text{Cs}$  for the measurement stations with a good accuracy.

### 4.3 Deposition of $^{137}\text{Cs}$ in European countries in relation to the Atlas

In this section the atmospheric budget and deposition patterns of  $^{137}\text{Cs}$  are assessed taking into consideration the contributions of different removal processes (i.e. particle sedimentation, dry and wet deposition, through large-scale and convective precipitation). The distribution of  $^{137}\text{Cs}$  deposited over Europe is shown in Fig. 10 (for the RG19L(S)), whereas in Fig. 11 the Atlas map is illustrated. Figs. 12–14 depict the respective runs with the real emission altitude (RG19L, RG39L and Z19L) for dry (top left panel), wet (top right panel) and total cumulative deposition (lower panel). In these figures, the same scale with the Atlas was used in order to better compare the results. Following the definition given by the International Atomic Energy Agency (IAEA, 2005, 2009), any area with activity larger than  $40\text{ kBq m}^{-2}$  is considered to be contaminated (see relevant red scale). Contamination means the presence of a radionuclide on a surface in

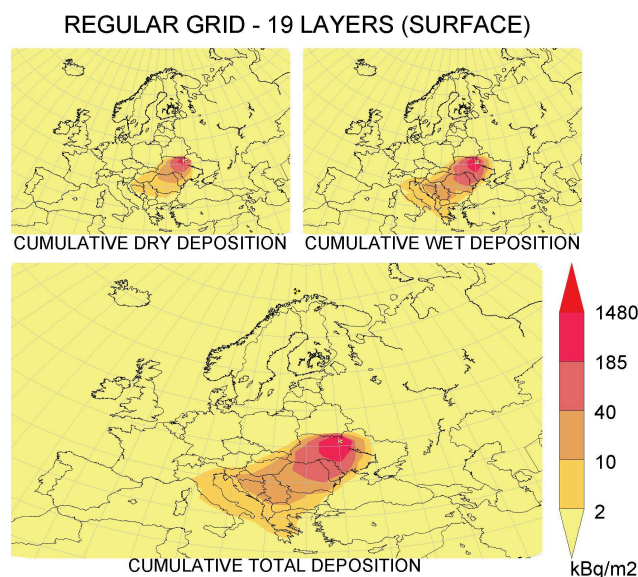


**Fig. 10.** Cumulative dry, wet and total deposition of  $^{137}\text{Cs}$  ( $\text{kBq m}^{-2}$ ) from the day of the accident (26 April 1986) until the end of 1986. Results of the simulation using the regular grid of the model for 19 vertical layers and accounting for source emissions to occur at the surface (RG19L(S)).

quantities larger than  $40\text{ kBq m}^{-2}$  for beta and gamma emitters ( $^{137}\text{Cs}$  is a gamma emitter). Since we integrate the deposition over the period after the accident until the end of 1986, the present results represent the cumulated contamination of this radionuclide.

The cumulative dry, wet and total deposition for 1986, estimated assuming that the emissions occurred at the surface (RG19L(S)), are depicted in Fig. 10. These data are presented here in order to certify and record the importance of the altitude of the emission in deposition after accidental releases. As can be seen from Fig. 10 the deposition of  $^{137}\text{Cs}$  is largely dependent upon the transport of the atmospheric burden. In the present situation where surface emissions assumed, the deposition was limited locally. It is mainly contingent from the surface southern winds and, following the dominant precipitation, it was deposited in Eastern Europe and the Balkan countries (Russia, Belarus, and Ukraine, ex-Czechoslovakia, Romania, Bulgaria, Greece and ex-Yugoslavia). An example can be given for Kiev (Ukraine), which is the most densely populated city close to the damaged reactor (around 100 km). According to the Atlas (Fig. 11), the deposition of  $^{137}\text{Cs}$  in this location appeared to be of the order of  $10\text{--}40\text{ kBq m}^{-3}$ . However, the model predicted a deposition greater than  $1480\text{ kBq m}^{-3}$ . That would lead the official authorities to evacuate the city. Therefore, it would be of major importance to know all the information following a major event. It is unexpected what would have happened if the official authorities of the ex-USSR evacuated an area of several thousand inhabitants by mistake.



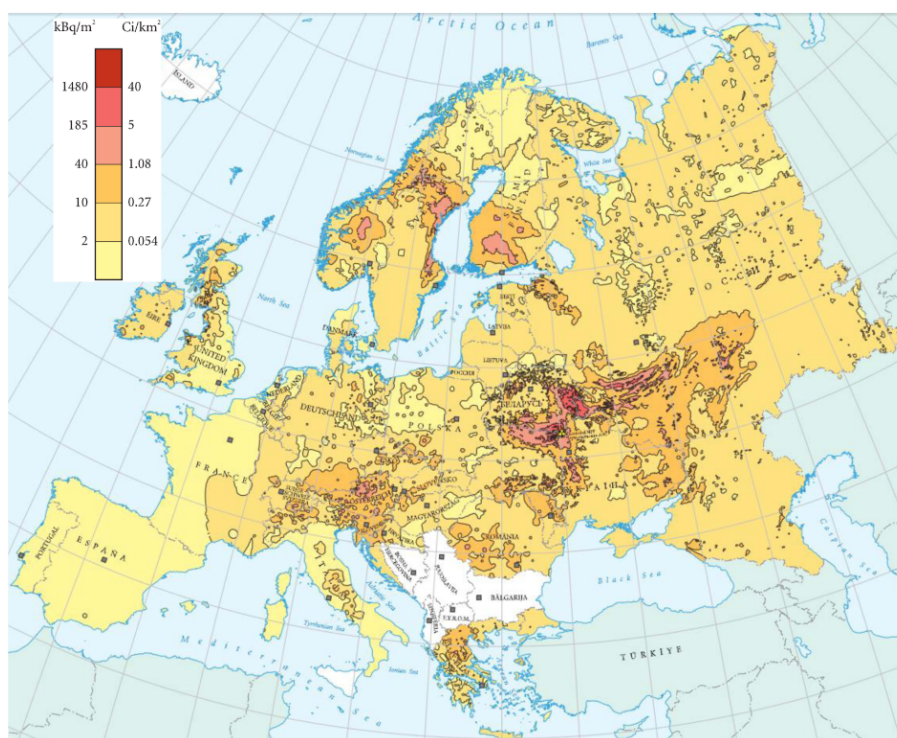


**Fig. 11.** The Atlas map depicting the total cumulative deposition of  $^{137}\text{Cs}$  throughout Europe as a result of the Chernobyl accident from all available data of the REM database corrected for radioactive decay to 10 May 1986. The map has been published in the “Atlas of caesium deposition on Europe after the Chernobyl accident” (De Cort et al., 1998).

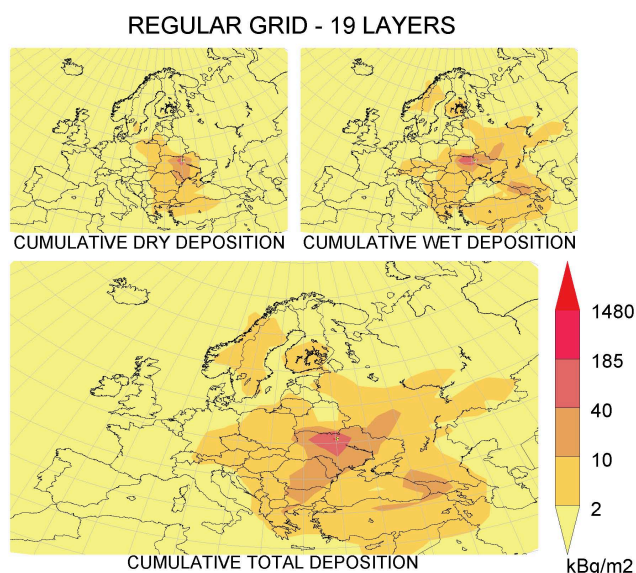


**Fig. 12.** Cumulative dry, wet and total deposition of  $^{137}\text{Cs}$  ( $\text{kBq m}^{-2}$ ) from the day of the accident (26 April 1986) until the end of 1986. Results of the simulation using the regular grid of the model for 19 vertical layers and accounting for the altitude of the emissions with respect to Table 1 (RG19L).

However, the measurements carried out by several accredited laboratories throughout Europe showed that there was transport to many other countries (Fig. 11). A more reliable deposition of  $^{137}\text{Cs}$  is reflected by the second run of the model, where  $^{137}\text{Cs}$  in the real emission altitude was injected (RG19L). The results are shown in Fig. 12. The transport as well as the dry deposition of  $^{137}\text{Cs}$  occurred also throughout Northern European countries especially in the first months after the accident. In addition, the observed precipitation resulted in deposition of higher amounts of  $^{137}\text{Cs}$  in specific areas of Sweden and Finland. However, a comparison of the total cumulative deposition of  $^{137}\text{Cs}$  simulated by the model to the observed one (De Cort et al., 1998, Fig. 11) showed that the levels of  $^{137}\text{Cs}$  deposition are overestimated over Central Europe. The Atlas indicates total deposition inventories of less than  $10 \text{ kBq m}^{-2}$ , whereas the total deposition inventories estimated in the model were found between 10 and  $40 \text{ kBq m}^{-2}$ .

The depositional patterns of RG39L simulation of the Chernobyl accident (Fig. 13) are different. The model underestimates the radioactive contamination in the northern countries (in Finland and Sweden), although enhanced depositions were estimated more easterly. Despite these deficiencies the model managed to estimate the increased contamination in the Alpine environment. It has been reported (De Cort et al., 1998) and can be also seen here (Fig. 11) that

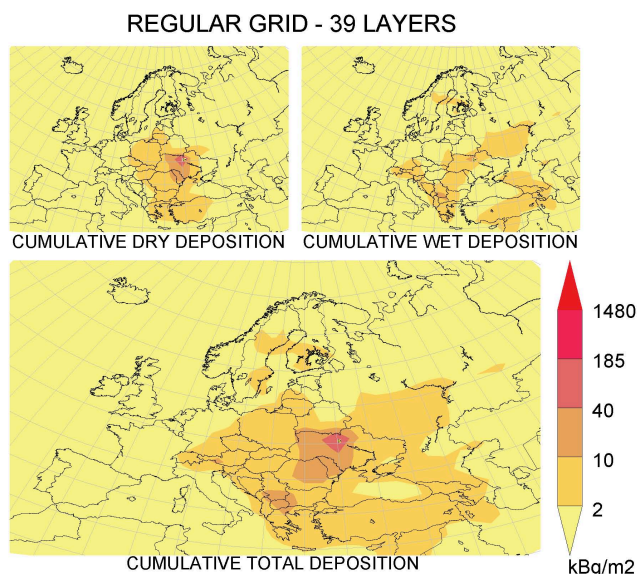


**Fig. 13.** Cumulative dry, wet and total deposition of  $^{137}\text{Cs}$  ( $\text{kBq m}^{-2}$ ) from the day of the accident (26 April 1986) until the end of 1986. Results of the simulation using the regular grid of the model for 39 vertical layers and accounting for the altitude of the emissions with respect to Table 1 (RG39L).

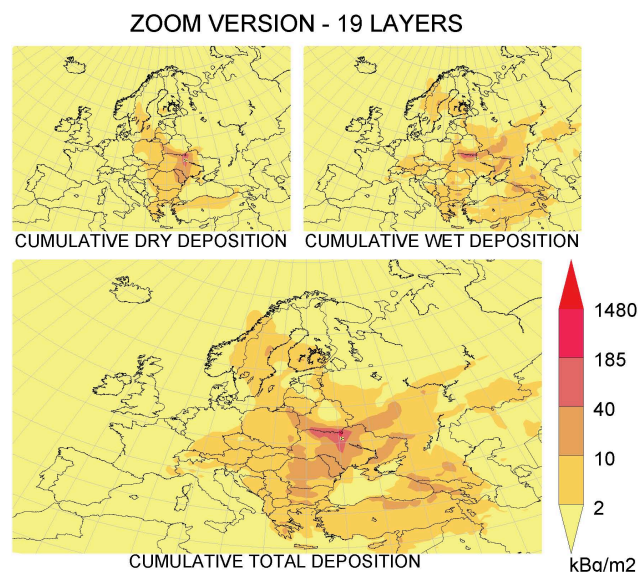


**Fig. 14.** Cumulative dry, wet and total deposition of  $^{137}\text{Cs}$  ( $\text{kBq m}^{-2}$ ) from the day of the accident (26 April 1986) until the end of 1986. Results of the simulation using the zoom-version of the model for 19 vertical layers and accounting for the altitude of the emissions with respect to Table 1.

$^{137}\text{Cs}$  have been deposited in the Alps after the accident, as a result of the intense precipitation. Moreover, the model also predicted effectively the deposition over North Greece.

As expected, the zoom-version of the model (Fig. 14) provides more discrete results of  $^{137}\text{Cs}$  deposition over Europe. The relative distribution of  $^{137}\text{Cs}$  deposition is similar to the Atlas, although underestimated, whereas some extremely high values of total cumulative deposition appeared in central Europe. The high deposition observed in Sweden is of the same magnitude and also, at the same location as those presented in Atlas. Another good example is the high total cumulative deposition observed in Russia (northeasterly of the Chernobyl NPP) (Carbol et al., 2003), which is predicted by the model accurately (see also Fig. 11). Finally, in Greece, enhanced depositions were observed in continental regions (Kritidis et al., 1990; Kritidis and Florou, 1995), and the model predicted them efficiently (see also Fig. 11). Despite the overestimations observed in Central Europe and underestimations in the highly contaminated areas, taking into account the heterogeneity of the direct measurements and the method used to create the Atlas map (inverse distance weighted interpolation method), one could note that the model gives remarkably good results.

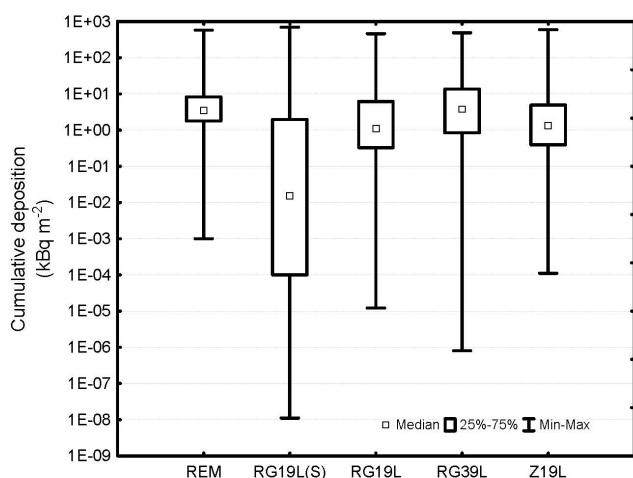
#### 4.4 Comparison with depositional observations reported by European countries

Figure S2 in the Supplement shows the location of the measurement stations where measurements of the cumulative total deposition were carried out and presented in the REM-

database. Over 4000 measurements from 20 European countries were used to evaluate and assess the modelling results in terms of the total cumulative deposition of  $^{137}\text{Cs}$ . However, no data from Ukraine, Belarus and Russia were available at the EU-JRC website. Table 4 shows the respective results of the statistical tests used in order to examine the relevance of the datasets (REM vs RG19L(S), RG19L, RG39L and Z19L, respectively) in contrast to the real-time measurements for  $^{137}\text{Cs}$  deposition. The Spearman correlation coefficient was estimated to range from 0.46 to 0.57 with 95 % confidence level ( $p < 0.05$ ), whereas the Kendall's tau ( $\tau$ ) rank correlation coefficient was estimated to vary between 0.33 and 0.42, (with 95 % confidence level,  $p < 0.05$ ) (Table 4), which shows the dependence between model datasets and observations. In fact, the results obtained from the different model runs (RG19L, RG39L and Z19L) were also contiguous presenting high coefficients ( $> 0.7$ ). Moreover, Fig. 15 depicts the Box and Whisker plots for the datasets in terms of the total cumulative deposition of  $^{137}\text{Cs}$ . There is an obvious trend of the model to underestimate the deposition of  $^{137}\text{Cs}$  in the countries examined taking into consideration the boxes corresponding to 25–75 % of the values, although these ranges were similar. For the comparisons of the model to observations of the deposition of  $^{137}\text{Cs}$ , reduced though nevertheless realistic agreement can be claimed, taking into account the inherent uncertainties based on the multitude and the complexity of the simulated removal processes (sedimentation, dry and wet deposition). In most cases there is close coincidence between the modelled and measured

**Table 4.** Comparison of the total cumulative deposition of  $^{137}\text{Cs}$  from the Chernobyl accident between the REM database and the different model versions used (RG19L(S), RG19L, RG39L and Z19L). Spearman Rank Order and Kendall Tau correlations ( $R^2$ ) between the datasets ( $N = 4266$ ) for 95 % confidence level ( $p < 0.05$ ).

	Spearman Rank Order correlation					Kendall Tau correlation					
	REM	RG19L(S)	RG19L	RG39L	Z19L	REM	RG19L(S)	RG19L	RG39L	Z19L	
REM	<b>1.00</b>	0.08	0.52	0.46	0.57	REM	<b>1.00</b>	0.05	0.39	0.33	0.42
RG19L(S)	0.08	<b>1.00</b>	0.23	0.37	0.25	RG19L(S)	0.05	<b>1.00</b>	0.16	0.26	0.18
RG19L	0.52	0.23	<b>1.00</b>	0.89	0.93	RG19L	0.39	0.16	<b>1.00</b>	0.74	0.81
RG39L	0.46	0.37	0.89	<b>1.00</b>	0.87	RG39L	0.33	0.26	0.74	<b>1.00</b>	0.71
Z19L	0.57	0.25	0.93	0.87	<b>1.00</b>	Z19L	0.42	0.18	0.81	0.71	<b>1.00</b>



**Fig. 15.** Box & Whisker plots of the cumulative total deposition of  $^{137}\text{Cs}$  obtained from the REM database and from the simulations using all the available versions of the model (RG19L(S), RG19L, RG39L and Z19L) for 1986. The plot depicts the smallest observation (sample minimum), lower quartile, median, upper quartile and the largest observation (sample maximum) ( $N = 4266$ ).

deposition inventories of  $^{137}\text{Cs}$ , although the simulated deposition fluxes underpredict measured ones by a factor of three in extreme cases. However, the model shows the arrival of high concentrations of radioactively contaminated aerosols at central European countries, and the same transport has been verified by previous models and certified by surface activity concentration measurements.

Figure S3 in the Supplement gives a more detailed view of the comparisons for each of the 20 European countries. It depicts linear regression scatter plots of the total  $^{137}\text{Cs}$  deposition based on individual measurements of each country (REM database) in descending order, in terms of the best linear fitting (1 : 1 dependence), as well as the respective calculated biases from the comparison with the observations. Given the large heterogeneity of the samples and the 50 % uncertainty of the emissions, the model results are in very good agreement with observations. The best performance was achieved for 14 countries (ex-Yugoslavia, Spain,

Hungary, Italy, Finland, Sweden, Greece, UK, Netherlands, Switzerland, Belgium, Germany, Norway and France) with correlation coefficients between 0.4 and 0.9, whereas the estimated average bias was  $-0.81 \pm 0.15$  for the RG19L run and the Z19L run and lower for the 39 level run ( $-0.25 \pm 0.91$ ). This seems very convenient if compared with other model assessments, which have showed biases around 1.3 for the total deposition of  $^{137}\text{Cs}$  (e.g. Brandt et al., 2002). Some discrepancies were observed in countries near the Chernobyl site (Romania, Poland, and ex-Czechoslovakia) and, also underestimations in Denmark, Ireland and Austria, while raw data from Ukraine, Belarus and Russia were unavailable from the public database. An important issue that should be stated here, regarding the data of  $^{137}\text{Cs}$  deposition from the REM database, is the fact that these data refer to total deposition of  $^{137}\text{Cs}$  over Europe, which means that the respective deposition from global atmospheric weapon testing, as well as other regional releases (e.g. Sellafield in Great Britain, Mayak in Urals, local releases from fuel fabrication, etc.) are included in the measurements. We believe that the observed underestimation of the model might be due to the fact that they have been more intensely affected by other releases (e.g. the background of  $^{137}\text{Cs}$  in central Europe prior to Chernobyl has been estimated to be greater than  $3 \text{ kBq m}^{-2}$ ). Finally, the precipitation fields were examined in order to assess if the observed difference in the deposition of  $^{137}\text{Cs}$  could be owed to a non-realistic wet deposition. For this reason, the relative difference between ERA40 ( $2.5^\circ \times 2.5^\circ$ ) precipitation and the one used by the LMDZ ( $0.66^\circ \times 0.51^\circ$ ) were calculated for 1986. We estimate an average discrepancy of 8 % in an area of  $700 \times 700 \text{ km}$ , which increases to 10 % in an area of  $3000 \times 3000 \text{ km}$  (all centred over the plant), which is very small and, hence, it is not expected to affect wet processes. The data for the precipitation comparison can be found in the Supplement, Figs. S4–S7.

## 5 Conclusions

The atmospheric cycle of  $^{137}\text{Cs}$  using LMDZORINCA model has been evaluated against real time measurements



of  $^{137}\text{Cs}$  from the Chernobyl accident in 1986. The model is based on a combination of the aerosol module INCA, the general circulation model LMDz and the global vegetation model ORCHIDEE. The conclusions are based on comparisons with measurements both from the REM database and from the Chernobyl Atlas. Simulations of the Chernobyl accident showed that comprehensive tracer models are powerful tools for estimating the activity concentrations and depositions after accidental scenarios.

According to the comparison between model and observations, the most sufficient results were obtained when the highest horizontal resolution of the model was used (Z19L run). Specifically, this model version managed to predict the radioactive contamination in most of the regions alike to Atlas. Except for higher coefficients and smaller biases from the comparison with the observations, for every variable examined (e.g. atmospheric activity concentrations, cumulative deposition of  $^{137}\text{Cs}$  etc.), a better resolved map similar to Atlas was obtained. However, there is a general trend for underestimation in the deposition, which could be attributed to the prevailing environmental processes and the large uncertainties of the source term, as well as to the background deposition of  $^{137}\text{Cs}$  from releases occurred prior to the accident that the model do not account for. The high vertical resolution of 39 levels can be useful only when the exact injection altitude is known. The increased number of levels in the boundary layer resulted in a different dispersion and deposition of  $^{137}\text{Cs}$ . When a moderate vertical resolution was used (19 layers in the RG19L run) the results were better. The accurate knowledge of the height of the emission is crucial in order to obtain credible transport and deposition of  $^{137}\text{Cs}$ . The resulting transport and deposition, when surface emissions were assumed, appeared to be local event in comparison to what really happened after the accident.

In all realistic situations studied (presenting the real ignition altitude) an ecological half-life of 6–9 days was estimated for the global atmospheric burden of  $^{137}\text{Cs}$ . In fact, previous modelling studies give global average half-lives of aerosols in the atmosphere on the order of 3–7 days, whereas for the Chernobyl and the recent Fukushima NPP accident a maximum of 10 days has been reported.

In addition, the arrival times of  $^{137}\text{Cs}$  in the model in comparison with the observations showed satisfactory correlations (0.46–0.65). Expected lack of dependence was estimated when surface emissions were assumed. The model is able to simulate and predict the development of the specific activity fields with high efficiency, although rarely underestimated. This is expected taking into account the uncertainties of the source term, the deposition processes and the heterogeneity in the samples. However, statistical tests applied to the respective datasets proved a likely dependence.

A general conclusion is that the high resolved grid gives results that track closely the observations, especially in the first days of the emissions. This imposes the essential usage of modelling applications as tools for the decision makers,

given that the first days of a nuclear accident are very important for life, in terms of addressing the appropriate evacuation criteria for the radiation protection of the population.

There is a critical need for open data policy after accidental releases. It is a pity that no data from all European countries are present in the public section of the REM database. The paper shows the importance of knowing the emission height of the source in such studies and how much it affects the dispersion and deposition of  $^{137}\text{Cs}$ . However, only speculations can be made about the real altitude where  $^{137}\text{Cs}$  was injected in the atmosphere and therefore, an uncertainty of 50% is always used in the case of Chernobyl. Nowadays, the existence of several modelling tools is able to predict the overall details of the emission after a NPP accident (e.g. using inverse modelling, Stohl et al., 2012). Knowing the exact core inventory by the official authorities or the real emissions during the first days, these dispersion models are able to predict the fate of the radioactive fallout. It is important that such an effort has been made after the recent accident in Japan where the IAEA has created a website with different databases for the Japanese authorities.

**Supplementary material related to this article is available online at:** <http://www.atmos-chem-phys.net/13/7183/2013/acp-13-7183-2013-supplement.zip>.

*Acknowledgements.* The authors would like to appreciate the funding source of the project (GIS Climat-Environnement-Société, <http://www.gisclimat.fr/projet/radioclimfire>). This work was granted access to the HPC resources of [CCRT/TGCC/CINES/IDRIS] under the allocation 2012-t2012012201 made by GENCI (Grand Equipement National de Calcul Intensif). Acknowledgements are also owed to Patrick Brockman who initiated us in the secrets of Ferret Analysis Scripting Toolbox and to the National Oceanic and Atmospheric Administration – Pacific Marine Environmental Laboratory (NOAA-PMEL) which created and shared the tool in public. The authors would like to acknowledge the Alfred Wegener Institute for Polar and Marine Research (AWI) and the Unidata community, as well, for releasing in public the free software Ocean Data View (ODV) and Integrated Data Viewer (IDV), respectively.

Edited by: P. Jöckel



The publication of this article is financed by CNRS-INSU.

## References

- Albergel, A., Martin, D., Strauss, B., and Gros, J.-M.: The Chernobyl accident: Modelling of dispersion over Europe of the radioactive plume and comparison with air activity measurements, *Atmos. Environ.*, 22, 2431–2444, 1988.
- ApSimon, H. M., Goddard, A. J. H., and Wrigley, J.: Long-range atmospheric dispersion of radioisotopes. The MESOS model, *Atmos. Environ.*, 19, 113–125, 1985.
- ApSimon, H. M., Wilson, J. J. N., and Scott, P. A.: Assessment of the Chernobyl release in the immediate aftermath of the accident, *Nucl. Energy*, 26, 295–301, 1987.
- Balkanski, Y. J., Jacob, D. J., Arimoto, R., and Kritiz, M. A.: Distribution of  $^{222}\text{Rn}$  over the North Pacific: Implications for continental influences, *J. Atmos. Chem.*, 14, 353–371, 1992.
- Ballestra, S. B., Holm, E., Walton, A., and Whitehead, N. E.: Fall-out deposition at Monaco following the Chernobyl accident, *J. Environ. Radioactiv.*, 5, 391–400, 1987.
- Bonelli, P., Calori, G., and Finzi, G.: A fast long-range transport model for operational use in episode simulation. Application to the Chernobyl accident, *Atmos. Environ.*, 26, 2523–2535, 1992.
- Brandt, J., Christensen, J. H., and Frohn, L. M.: Modelling transport and deposition of caesium and iodine from the Chernobyl accident using the DREAM model, *Atmos. Chem. Phys.*, 2, 397–417, doi:10.5194/acp-2-397-2002, 2002.
- Cambray, R. S., Cawse, P. A., Garland, J. A., Gibson, J. A. B., Johnson, P., Lewis, G. N. J., Newton, D., Salmon, L., and Wade, B. O.: Observations on radioactivity from the Chernobyl accident, *Nucl. Energy*, 26, 77–101, 1987.
- Carbol, P., Solatie, D., Erdmann, N., Nysten, T., and Betti, M.: Deposition and distribution of Chernobyl fallout fission products and actinides in a Russian soil profile, *J. Environ. Radioactiv.*, 68, 27–46, 2003.
- Choi, S. C.: Test of equality of dependent correlations, *Biometrika*, 64, 645–647, 1977.
- Christensen, D.: Fast algorithms for the calculation of Kendall's  $\tau$ , *Computation. Stat.*, 20, 51–62, 2005.
- De Cort, M., Dubois, G., Fridman, Sh. D., Germenchuk, M. G., Izrael, Yu. A., Janssens, A., Jones, A. R., Kelly, G. N., Kvasnikova, E. V., Matveenko, I. I., Nazarov, I. M., Pokumeiko, Yu. M., Sitak, V. A., Stukin, E. D., Tabachny, L. Ya., Tsaturov, Yu. S., and Avdyushin, S. I.: Atlas of caesium deposition on Europe after the Chernobyl accident, Luxembourg, Office for Official Publications of the European Communities 1998, ISBN 92-828-3140-X, Catalogue number CG-NA-16-733-29-C. EUR 16733, 1–63, 1998.
- Desiato, F.: A long-range dispersion model evaluation study with Chernobyl data, *Atmos. Environ.*, 26, 2805–2820, 1992.
- Devell, L., Guntay, S., and Powers, D. A.: The Chernobyl reactor accident source term. Development of a consensus view, NEA/CSNI/R(95)24, OECD Nuclear Energy Agency, Paris, 1996.
- ECMWF: ERA-40, forty-year European re-analysis of the global atmosphere, available at: <http://www.ecmwf.int/products/data/archive/descriptions/e4>, 2002.
- Elliassen, A.: The OCDE study of long range transport or air pollutants: long-range transport modelling, *Atmos. Environ.*, 12, 479–487, 1978.
- Elliassen, A. and Saltbones, J.: Modelling of long-range transport of sulphur over Europe: a two-year model run and some model experiments, *Atmos. Environ.*, 17, 1457–1473, 1983.
- Hass, H., Memmesheimer, M., Geiss, H., Jakobs, H. J., Laube, M., and Ebel, A.: Simulation of the Chernobyl radioactive cloud over Europe using EURAD model, *Atmos. Environ.*, 24, 673–692, 1990.
- Hatano, Y., Hatano, N., Amano, H., Ueno, T., Sukhoruchkin, A. K., and Kazakov, S. V.: Aerosol migration near Chernobyl: long-term data and modelling, *Atmos. Environ.*, 32, 2587–2594, 1998.
- Hourdin, F. and Issartel, J. P.: Sub-surface nuclear tests monitoring through the CTBT xenon network, *Geophys. Res. Lett.*, 27, 2245–2248, 2000.
- Huneus, N., Schulz, M., Balkanski, Y., Griesfeller, J., Prospero, J., Kinne, S., Bauer, S., Boucher, O., Chin, M., Dentener, F., Diehl, T., Easter, R., Fillmore, D., Ghan, S., Ginoux, P., Grini, A., Horowitz, L., Koch, D., Krol, M. C., Landing, W., Liu, X., Mahowald, N., Miller, R., Morcrette, J.-J., Myhre, G., Penner, J., Perlwitz, J., Stier, P., Takemura, T., and Zender, C. S.: Global dust model intercomparison in AeroCom phase I, *Atmos. Chem. Phys.*, 11, 7781–7816, doi:10.5194/acp-11-7781-2011, 2011.
- International Atomic Energy Agency (IAEA): Regulations for the Safe Transport of Radioactive Material, IAEA Safety Requirements, no. TS-R-1, Vienna, 2005.
- International Atomic Energy Agency (IAEA): Environmental consequences of the Chernobyl accident and their remediation: Twenty years of experience. Report of the Chernobyl Forum Expert Group “Environment”, Radiological Assessment Reports Series, Vienna, 2006.
- International Atomic Energy Agency (IAEA): Regulations for the Safe Transport of Radioactive Material, IAEA Safety Requirements, no. TS-R-1, Vienna, 2009.
- Ishikawa, H.: Evaluation of the effect of horizontal diffusion on the long-range atmospheric transport simulation with Chernobyl data, *J. Appl. Meteorol.*, 34, 1653–1665, 1995.
- Jacob, D. J., Prather, M. J., Wofsy, S. C., and McElroy M. B.: Atmospheric distribution of  $^{85}\text{Kr}$  simulated with a general circulation modelJGR, *J. Geophys. Res.*, 92, 6614–6626, 1987.
- Jacob, D. J., Prather, M. J., Rasch, P. J., Shia, R. L., Balkanski, Y. J., Beagley, S. R., Bergmann, D. J., Blackshear, W. T., Brown, M., Chiba, M., Chipperfield, M. P., De Grandpré, J., Dignon, J.E., Feichter, J., Genthon, C., Grose, W. L., Kasibhatla, P. S., Köhler, I., Kritiz, M. A., Law, K., Penner, J. E., Ramonet, M., Reeves, C. E., Rotman, D. A., Stockwell, D. Z., Van Velthoven, P. F. J., Verver, G., Wild, O., Yang, H., and Zimmermann, P.: Evaluation and intercomparison of global atmospheric transport models using  $^{222}\text{Rn}$  and other short-lived tracers, *J. Geophys. Res.*, 102, 5953–5970, 1997.
- Klug, W., Graziani, G., Grippa, G., Pierce, D., and Tassone, C.: Evaluation of long range atmospheric transport models using environmental radioactivity data from the Chernobyl accident, The ATMES Report, Elsevier Applied Science, London and New York, 366 pp., 1992.
- Koch, D., Schulz, M., Kinne, S., McNaughton, C., Spackman, J. R., Balkanski, Y., Bauer, S., Berntsen, T., Bond, T. C., Boucher, O., Chin, M., Clarke, A., De Luca, N., Dentener, F., Diehl, T., Dubovik, O., Easter, R., Fahey, D. W., Feichter, J., Fillmore, D., Freitag, S., Ghan, S., Ginoux, P., Gong, S., Horowitz, L., Iversen, T., Kirkevåg, A., Klimont, Z., Kondo, Y., Krol, M., Liu, X., Miller, R., Montanaro, V., Moteki, N., Myhre, G., Penner, J. E., Perlwitz, J., Pitari, G., Reddy, S., Sahu, L., Sakamoto, H.,

- Schuster, G., Schwarz, J. P., Seland, Ø., Stier, P., Takegawa, N., Takemura, T., Textor, C., van Aardenne, J. A., and Zhao, Y.: Evaluation of black carbon estimations in global aerosol models, *Atmos. Chem. Phys.*, 9, 9001–9026, doi:10.5194/acp-9-9001-2009, 2009.
- Kornberg, H. A.: The use of element-pairs in radiation hazard assessment, *Health Phys.*, 6, 46–62, 1961.
- Kristiansen, N. I., Stohl, A., and Wotawa, G.: Atmospheric removal times of the aerosol-bound radionuclides  $^{137}\text{Cs}$  and  $^{131}\text{I}$  measured after the Fukushima Dai-ichi nuclear accident – a constraint for air quality and climate models, *Atmos. Chem. Phys.*, 12, 10759–10769, doi:10.5194/acp-12-10759-2012, 2012.
- Kritidis, P.: Radioactive contamination of the environment, in: *Ourselves and Radioactivity*, University of Crete Publications, edited by: Verganelakis, A., Kritidis, P., Economou, L., Papazoglou, I., Papanikolaou, E., Sideris, L., and Simopoulos, T., Heraklion, Greece, 235–270, 1989 (in Greek).
- Kritidis, P. and Florou, H.: Environmental study of radioactive caesium in Greek lake fish after the Chernobyl accident, *J. Environ. Radioactiv.*, 28, 285–293, 1995.
- Kritidis, P., Florou, H., and Papanicolaou, E.: Delayed and late impact of the Chernobyl accident on the Greek environment, *Radiat. Prot. Dosim.*, 30, 187–190, 1990.
- Lange, R., Dickerson, M. H., and Gudiksen, P. H.: Dose estimates from the Chernobyl accident, *Nucl. Technol.*, 82, 311–323, 1988.
- Lee, D.S., Nemitz, E., Fowler, D., and Kingdon, R.D.: Modelling atmospheric mercury transport and deposition across Europe and the UK, *Atmos. Environ.*, 35, 5455–5466, 2001.
- Lelieveld, J., Kunkel, D., and Lawrence, M. G.: Global risk of radioactive fallout after major nuclear reactor accidents, *Atmos. Chem. Phys.*, 12, 4245–4258, doi:10.5194/acp-12-4245-2012, 2012.
- Mattsson, S. and Vesanen, R.: Patterns of Chernobyl fallout in relation to local weather conditions, *Environ. Int.*, 14, 177–180, 1988.
- Morino, Y., Ohara, T., and Nishizawa, M.: Atmospheric behavior, deposition, and budget of radioactive materials from the Fukushima Daiichi nuclear power plant in March 2011, *Geophys. Res. Lett.*, 38, L00G11, doi:10.1029/2011GL048689, 2011.
- Oliví, D. J. L., Cariolle, D., Teysse, H., Salas, D., Voldoire, A., Clark, H., Saint-Martin, D., Michou, M., Karcher, F., Balkanski, Y., Gauss, M., Dessens, O., Koffi, B., and Sausen, R.: Modelling the climate impact of road transport, maritime shipping and aviation over the period 1860–2100 with an AOGCM, *Atmos. Chem. Phys.*, 12, 1449–1480, doi:10.5194/acp-12-1449-2012, 2012.
- Peplow, M.: Counting the dead (special report about the death toll of the Chernobyl accident), *Nature*, 440, 982–983, 2006.
- Piedelievre, J. P., Musson-Genon, L., and Bompay, F.: MEDIA – An Eulerian model for atmospheric dispersion: First validation on the Chernobyl release, *J. Appl. Meteorol.*, 29, 1205–1220, 1990.
- Potiriadis, C., Kolovou, M., Clouvas, A., and Xanthos, S.: Environmental radioactivity measurements in Greece following the Fukushima Daichi nuclear accident, *Radiat. Prot. Dosim.*, 150, 441–447, 2011.
- Prather, M., McElroy, M., Wofsy, S., Russell, G., and Rind, D.: Chemistry of the global troposphere: Fluorocarbons as tracers of air motion, *J. Geophys. Res.*, 92, 6579–6613, 1987.
- Quélo, D., Krysta, M., Bocquet, M., Isnard, O., Minier, Y., and Sportisse, B.: Validation of the Polyphemus platform on the ETEX, Chernobyl and Algeciras cases, *Atmos. Environ.*, 41, 5300–5315, 2007.
- Ritchie, J. C. and McHenry, J. R.: Application of radioactive fallout cesium-137 for measuring soil erosion and sediment accumulation rates and patterns: A review, *J. Environ. Qual.*, 19, 215–233, 1990.
- Salvadori, G., Ratti, S. P., and Belli, G.: Modelling the Chernobyl radioactive fallout (II): A multifractal approach in some European countries, *Chemosphere*, 33, 2359–2371, 1996.
- Sportisse, B.: A review of parameterizations for modelling dry deposition and scavenging of radionuclides, *Atmos. Environ.*, 41, 2683–2698, 2007.
- Stier, P., Feichter, J., Kinne, S., Kloster, S., Vignati, E., Wilson, J., Ganzeveld, L., Tegen, I., Werner, M., Balkanski, Y., Schulz, M., Boucher, O., Minikin, A., and Petzold, A.: The aerosol-climate model ECHAM5-HAM, *Atmos. Chem. Phys.*, 5, 1125–1156, doi:10.5194/acp-5-1125-2005, 2005.
- Stohl, A., Seibert, P., Wotawa, G., Arnold, D., Burkhart, J. F., Eckhardt, S., Tapia, C., Vargas, A., and Yasunari, T. J.: Xenon-133 and caesium-137 releases into the atmosphere from the Fukushima Dai-ichi nuclear power plant: determination of the source term, atmospheric dispersion, and deposition, *Atmos. Chem. Phys.*, 12, 2313–2343, doi:10.5194/acp-12-2313-2012, 2012.
- Szopa, S., Balkanski, Y., Cozic, A., Deandrea, C., Dufresne, J.-L., Hauglustaine, D., Lathiere, J., Schulz, M., Vuolo, R., Yan, N., Marchand, M., Bekki, S., Cugnet, D., Idelkadi, A., Denvil, S., Foujols, M.-A., Caubel, A., and Fortems-Cheiney, A.: Aerosol and Ozone changes as forcing for Climate Evolution between 1850 and 2100, *Clim. Dynam.*, in press, doi:10.1007/s00382-012-1408-y, 2012.
- Waight, P., Métivier, H., Jacob, P., Souchkevitch, G., Viktorsson, C., Bennett, B., Hance, R., Kumazawa, S., Kusumi, S., Bouville, A., Sinnaeve, J., Ilari, O., and Lazo, E.: Chernobyl Ten Years On. Radiological and Health Impact. An Assessment by the NEA Committee on 10 Radiation Protection and Public Health, November 1995, OECD Nuclear Agency, <http://www.nea.fr/>, 74 pp., 1995.
- Woodhead, D. S.: Levels of radioactivity in the marine environment and the dose commitment to the marine organisms, I.A.E.A. – S.M. 158/31, Vienna, 1973.
- Yoschenko, V. I., Kashparov, V. A., Protsak, V. P., Lundin, S. M., Levchuk, S. E., Kadygrib, A. M., Zvarich, S. I., Khomutinin, Yu. V., Maloshtan, I.M., Lanshin, V. P., Kovtun, M. V., and Tschiersch, J.: Resuspension and redistribution of radionuclides during grassland and forest fires in the Chernobyl exclusion zone: part I. Fire experiments, *J. Environ. Radioactiv.*, 86, 143–163, 2006.